



## Luminescent PEO Coatings on Aluminum

Aleksejs Zolotarjovs,<sup>z</sup> Krisjanis Smits, Anete Krumina, Donats Millers, and Larisa Grigorjeva

Institute of Solid State Physics, University of Latvia, Riga LV-1063, Latvia

Results show the possibilities of pore filling approach to modify alumina coatings with various materials in order to enhance coating optical (or other) properties and develop new functional materials; as well as demonstrate novel alumina phase transition detection approach. Luminescent PEO coatings were produced on aluminum surface using pore-filling method. Three stage process was developed to modify alumina coating in order to enhance its luminescent properties.  $\text{Eu}^{3+}$  recharging to  $\text{Eu}^{2+}$  followed by significant (up to 10 times) total luminescence intensity increase was observed, Eu ion presence evaluated in final coating by measuring fast decay kinetics. Structure of obtained coatings was analyzed using XRD and FTIR spectroscopy indicating presence of  $\eta$ -alumina phase.

© 2016 The Electrochemical Society. [DOI: 10.1149/2.0401609jss] All rights reserved.

Manuscript submitted July 6, 2016; revised manuscript received August 3, 2016. Published August 18, 2016.

Alumina coatings on aluminum surface are widely used in various technical applications to improve metal mechanical and chemical properties. A wide variety of technological processes can be used to produce such coatings with the most straight-forward approach being electrochemical deposition. With the recent technological advances Plasma Electrolytic Oxidation (PEO) became a perspective method to make thick (in order of  $100 \mu\text{m}^1$ ) ceramic coatings using high voltage and current to achieve spark discharges through dielectric layer thus producing plasma exhibiting high temperature and pressure. With temperatures up to  $10^4 \text{K}^2$  it is possible to produce complex metal oxides including  $\alpha$ -alumina phase coatings on aluminum<sup>3</sup> having great mechanical and thermal stability<sup>4</sup> as well as good corrosion resistance.<sup>5</sup> Since the process can be applied to various valve metals in different shapes, one can find various publications regarding PEO on Zn,<sup>6</sup> Mg,<sup>7</sup> Ti<sup>8,9</sup> and even on highly-porous aluminum networks.<sup>10</sup>

The development of luminescent coatings is of interest due to various practical applications in different fields. The spectral distribution of emission from Eu ions can be used for coating phase determination,<sup>11</sup> light conversion<sup>12</sup> and many other applications. Although there are studies producing luminescent coatings with anodization by either using modified electrolyte<sup>13</sup> or filling small ( $10\text{--}400 \text{nm}^{14}$ ) highly organized pores with luminescent materials<sup>15</sup> (as part of using porous coatings as a template for nanowire growth), the studies of producing luminescent PEO coatings are not so common. Recently, a first paper on luminescent coating preparation was published,<sup>16</sup> describing a way to produce coatings with bright  $\text{Eu}^{2+}$  or  $\text{Eu}^{3+}$  luminescence using high purity Al doped with Eu. Despite the good results, the main disadvantage of this method is the use of Eu doped Al alloy, which drastically limits potential practical applications due to the cost of raw materials as well as unnecessary incorporation of Eu in the whole metal volume, where only surface layer is used; however, results give the insight of coating development during PEO process and their possible applications.

Later, a different approach was used to produce luminescent zirconia coatings on zirconium. Approach is based on the principle of modifying electrolyte and was previously used to enhance various coating properties (as an example, carbon nanotubes for improved corrosion resistance<sup>17</sup>); however, for enhancement of luminescence properties of zirconia coatings,  $\text{Sm}_2\text{O}_3$  or  $\text{Eu}_2\text{O}_3$  powders were added to electrolyte to dope zirconia with  $\text{Sm}^{3+18}$  and  $\text{Eu}^{3+19}$  ions respectively. In addition, the same principle was applied to produce Eu doped  $\text{TiO}_2$  coatings<sup>20</sup> and  $\text{Eu}^{3+}$ ,  $\text{Sm}^{3+}$  doped  $\text{Nb}_2\text{O}_5$  coatings.<sup>21</sup>

To broaden possible technological applications commercially available aluminum alloy must be used as a base material as well as more economically viable doping technology should be developed. One of alternative methods for dopand implementation in coatings could be pore creation followed by their filling with different materials and applying PEO process to the sample.

The aim of this work is to broaden possibilities of PEO process for modified luminescent coating production using pore filling technique therefore reducing material cost and increasing process flexibility.

### Experimental

**Samples and preparation.**—"Commercially pure" 99.5% aluminum 1050 was used in all experiments. All samples were water jet cut from 2 mm thick non-polished aluminum plate. The final sample size is  $25 \times 25 \times 2 \text{mm}$  (total area –  $14.5 \text{cm}^2$ ). The whole sample preparation process can be divided in 3 stages: porous alumina coating preparation, filling pores with  $\text{Eu}(\text{OH})_3$  and PEO coating production.

**First stage.**—Before any electrochemical process aluminum samples were polished using SiC sandpapers followed with  $\text{Cr}_2\text{O}_3$  and diamond paste and rinsed off with acetone. To produce porous alumina coating custom 5 kW bipolar pulse electric generator ELGOO PEO v3 (Applied Electronics labs) was used. To achieve repeatability and ease of control, unique software LPEO v2.8 was used providing the control of electrolysis process. Bipolar pulsed (10 kHz) voltage-limited algorithm was used, which can be divided in three steps: firstly, positive voltage held at 350 V (V-held at 400 V (or less), current unlimited) for 5 minutes, secondly linearly increased positive voltage from 350 V to 400 V in 5 minutes (keeping all the other parameters same), and lastly positive voltage held at 400 V for 5 minutes (keeping all the other parameters same). For counter-electrode Pt foil with a surface area of  $20 \text{cm}^2$  was used, spaced 2 cm from the sample. The electrolyte contained 2 g/L KOH, 7.5 g/L  $\text{Na}_3\text{PO}_4$  and 6 ml/L glycerine. All reactants soluted in high quality deionized water. Constantly stirred electrolyte was placed in a double-walled tempered glass reactor with active water cooling to keep a constant temperature. After the process, samples were washed with water and dried in air at room temperature. During the first stage the porous coating on aluminum sample was obtained.

**Second stage.**—To fill the pores  $\text{Eu}(\text{OH})_3$  powder was used. The powder was prepared from Eu nitrate using sol-gel method: 10 g/L  $\text{Eu}(\text{NO}_3)_3 + 120 \text{g/L}$  urea stirred in 100 ml of deionized water for 60 min at  $90^\circ\text{C}$ , then filtered and dried at room temperature. To fill the pores, a small amount of  $\text{Eu}(\text{OH})_3$  powder was grind in mortar for 10 minutes with addition of ethanol to keep particles from agglomerating, the resulting solution was dried at room temperature on top of the porous samples prepared in first stage and rinsed off with deionized water to remove excess powder.

**Third stage.**—A classic PEO process was performed on filled porous samples. The same Pt foil from first stage (2.1.1.) was used as a counter electrode. 1 L of deionized water with 2 g/L KOH was used as an electrolyte. Constant voltage-limited (with voltages up to 530 V and current density  $0.15 \text{A/cm}^2$ ) unipolar regime was used for the extended periods of time to achieve plasma discharges through coating.

<sup>z</sup>E-mail: alexeyzolotarjov@gmail.com

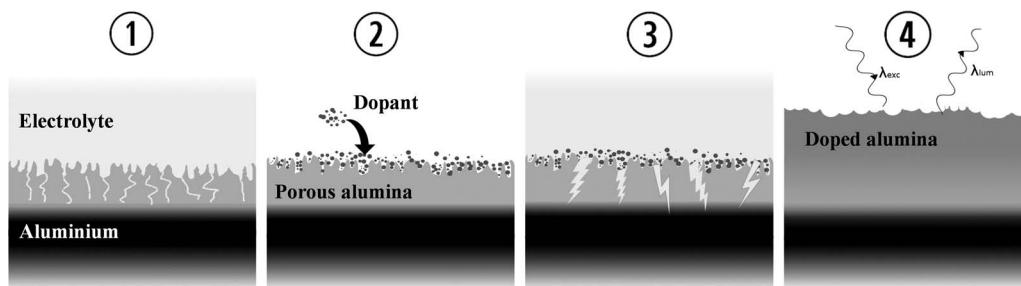


**Figure 1.** Schematic illustration of sample preparation process. 1 – porous alumina coating preparation, 2 – filling pores with particles, 3 – PEO process, 4 – final doped alumina coating.

To the author's knowledge, this pore-filling approach was never used before, especially for luminescent coating production. Authors believe that this approach can be used to implement various dopants in different coatings. The schematic illustration of preparation process is displayed in Fig. 1.

**Measurements.**—266 nm YAG laser was used as photoluminescence excitation source. The luminescence measurements were performed using Andor Shamrock B-303i spectrograph coupled with Andor DU-401A-BV CCD camera. For luminescence kinetics measurements the PMT H8259-02 (Hamamatsu) was used. Various optical filters were used to filter unused laser harmonics and ambient light.

SEM measurements were made on Phenom Pro scanning electron microscope.

Fourier Transform Infrared spectra was taken using Kubelka-Munk method on Bruker Vertex 80 V FTIR spectrometer.

X-ray diffraction spectra for crystalline structure studies were taken using PANalytical X'Pert Pro diffractometer.

## Results and Discussion

During the sample preparation, the main problem is reliability and repeatability of preparation process. While fully-programmable power supply was crucial in achieving electrochemical process repeatability, quality of surface polishing prior to first stage strongly affected the resulting porous coating. The pore diameter of obtained coatings varying from 0.8–2  $\mu\text{m}$  was estimated from SEM images (Fig. 2). In addition, the thickness of porous coating was estimated at 30  $\mu\text{m}$  with pore depth 500 nm and higher.

$\text{Eu}(\text{OH})_3$  powder prepared with sol-gel method was deposited on coatings (Fig. 2B). The SEM image shows the Eu powder distribution on coating, estimated grain size of powder varies from 300 nm to 2  $\mu\text{m}$  - mostly smaller than pore size, which keeps powder in place during rinsing with water, electrolyte and during PEO process itself.

By analyzing SEM images no evident surface morphology change on stage 3 was observed from incorporating Eu in coatings (Fig. 2C and 2D images).

Photoluminescence spectra excited with 266 nm laser were measured at every sample preparation stage. The spectra are presented on Fig. 3. Distinct  $\text{Eu}^{3+}$  (red) luminescence was observed from powder sample of  $\text{Eu}(\text{OH})_3$  corresponding to transitions from  $^5\text{D}_0$  level to  $^7\text{F}$  with the most intense line at 613 nm corresponding to  $^5\text{D}_0 \rightarrow ^7\text{F}_2$  transition.<sup>11</sup>

Wide intrinsic alumina luminescence peaking at 450 nm was observed from porous coating. After filling pores with  $\text{Eu}^{3+}$  powder, both intrinsic and  $\text{Eu}^{3+}$  luminescence was observed. (Fig. 3 green line).

After applying high voltage (third stage) to achieve plasma electric discharges  $\text{Eu}^{3+}$  luminescence maxima disappeared from spectra. Moreover, a new broad luminescence band appeared in blue region. Similar effect was observed in Ref. 16 where it was described as  $\text{Eu}^{3+}$  recharging to  $\text{Eu}^{2+}$ . The recharging to the  $\text{Eu}^{2+}$  might be related to the oxygen vacancies: to compensate the charge difference the Eu

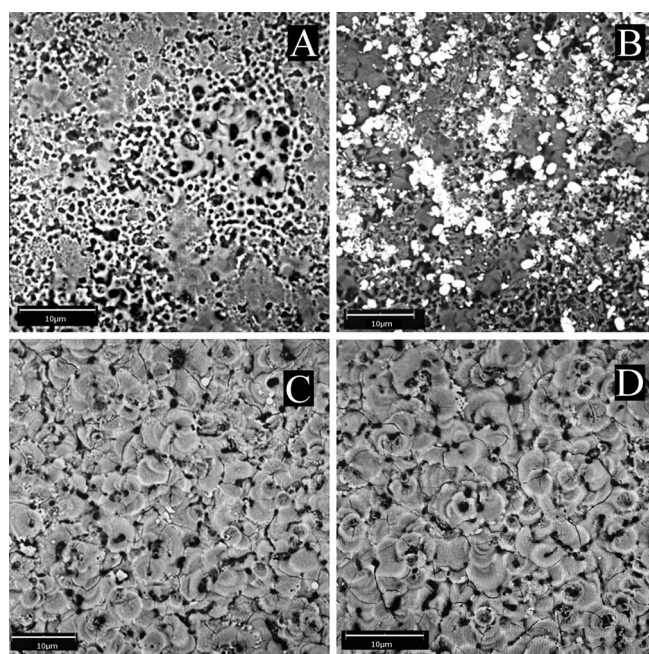


**Figure 2.** SEM images of prepared samples – A – clean pores after first stage, B – pores filled with  $\text{Eu}(\text{OH})_3$  after second stage, C – PEO ceramic coating after third stage (with Eu), D – PEO ceramic coating without Eu.

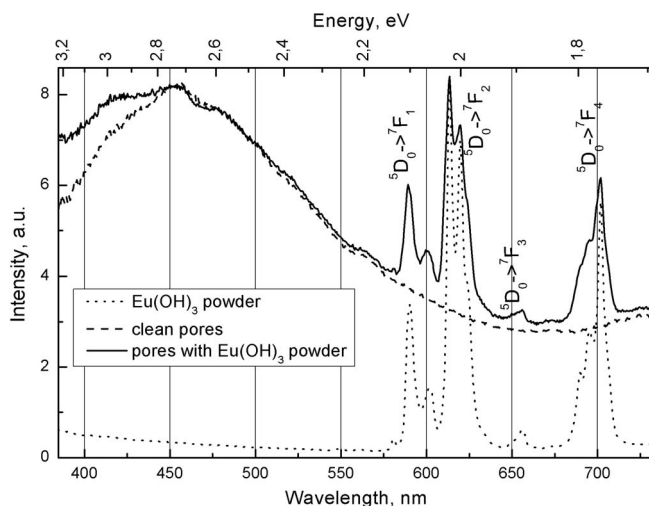


**Figure 3.** Photoluminescence of  $\text{Eu}(\text{OH})_3$  sol-gel powder, clean porous alumina coating and filled pores. Excitation wavelength – 266 nm.

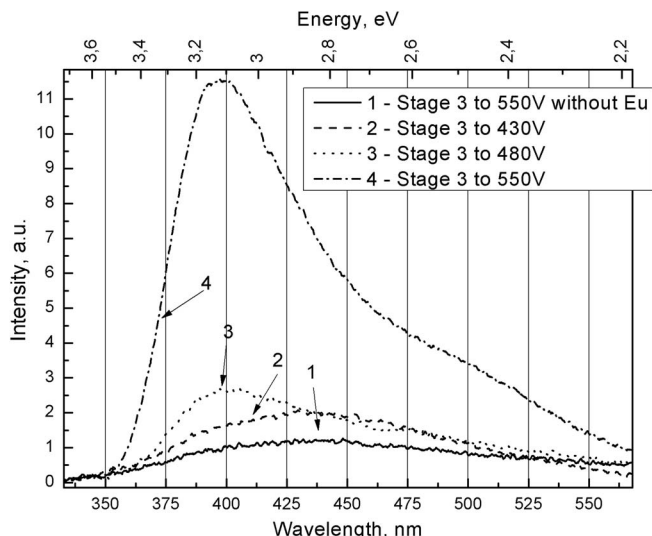


**Figure 4.** Luminescence spectra of obtained coatings after third stage. None of the presented sample exhibited  $\text{Eu}^{3+}$  luminescence (613 nm).

incorporates in divalent state, although additional XPS measurements are necessary to prove this assumption. The  $\text{Eu}^{2+}$  ion luminescence in blue region of spectra was also found in doped translucent alumina ceramics<sup>22</sup> as well as in different  $\text{Eu}^{2+}$ -doped alkaline-earth aluminates.<sup>23,24</sup> The position of peak is shifted to “blue” region and can be associated with weak crystal field. The resulting spectra of samples after 3-rd stage can be found in Fig. 4.

In addition to possible Eu recharging, photoluminescence intensity at 400 nm increased up to 10 times in comparison with undoped samples. It was observed that luminescence intensity growth correlates with applied PEO voltage to the sample. Fig. 5 shows 400 nm band photoluminescence intensity change as a function of applied voltage in third stage. Luminescence intensity increase starts with first anodic sparks (450 V) and saturates at 500 V. Unexpected plateau at 480–490 V was observed: by analyzing XRD and FTIR spectra authors assume that this is due to measurement error.

To evaluate  $\text{Eu}^{2+}$  ion luminescence the decay kinetics were measured. UV (266 nm) excitation source was used while the luminescence was measured at 470 nm and 410 nm to differentiate  $\text{Eu}^{2+}$  and intrinsic luminescence (refer to Fig. 4). All decay curves were normalized at 10 ns to remove laser pulse and fast component of luminescence. Decay kinetics curve of undoped sample can be ap-

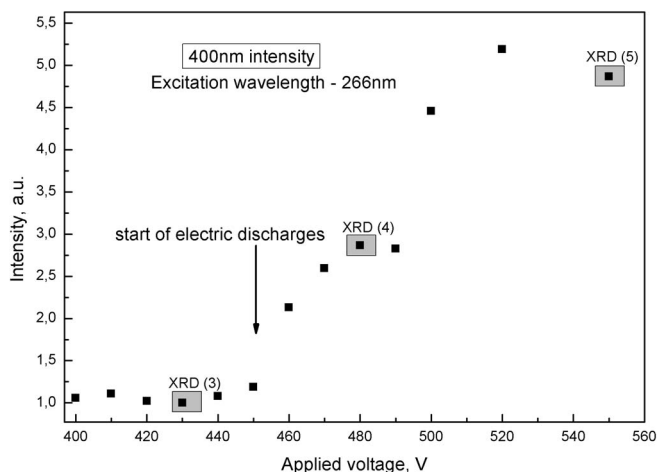


**Figure 5.** Photoluminescence intensity at 400 nm for various PEO voltages.

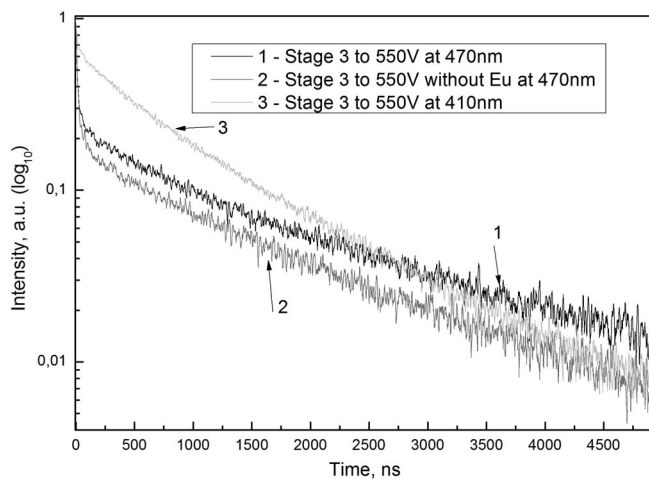


**Figure 6.** Luminescence decay kinetics of sample after third stage with Eu and without Eu.

proximated with two exponents with decay times 690 ns and 1.6  $\mu\text{s}$ , while the sample with Eu shows additional long component in order of 3  $\mu\text{s}$  (typical for partially forbidden  $\text{Eu}^{2+}$  transitions), although it is impossible to reliably approximate this complex curve with exponents. Decay kinetics are shown on Fig. 6.

For coating structure measurements, XRD spectra were taken (Fig. 7). In addition to Al lines (38.5 and 44.5 deg.) distinct magnesium silicate maxima (“b” lines on Fig. 7) were observed on clean Al 1050 sample as well as in all the other samples indicating various intermetallic phase particles in raw material.<sup>25</sup> While no change in XRD is present after the addition of porous alumina oxide; after 480 V (4, 5, 6 graphs on Fig. 7)  $\eta\text{-Al}_2\text{O}_3$  lines<sup>26</sup> appear (“a” lines on Fig. 6), indicating a cubic alumina phase with lattice constant  $a = 7.9320$ . No  $\alpha$ -alumina or  $\gamma$ -alumina phases were observed.<sup>3</sup>

By analyzing FTIR spectra (Fig. 8) one can see that, although  $\alpha$ -alumina lines (636, 590 and 443  $\text{cm}^{-1}$ )<sup>27</sup> were not observed, distinct spectral changes can be registered during PEO development. Wide spectral lines similar to amorphous alumina described in Ref. 27 can be found in long wavelength range of the spectrum in the samples with  $\eta\text{-Al}_2\text{O}_3$  structure.

As obtained spectra are of complex nature, further research should be conducted to extract more information.

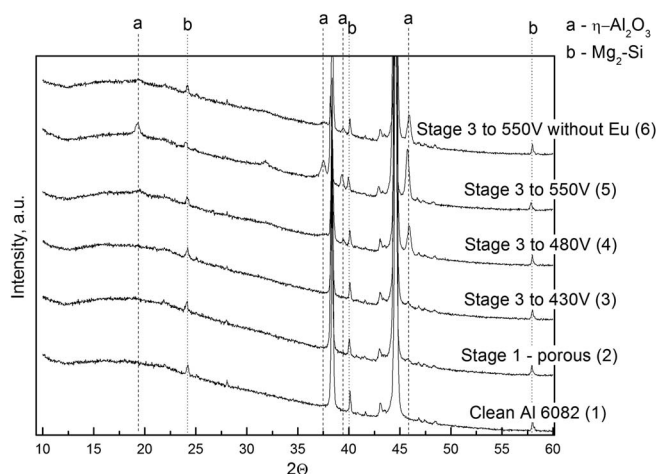


**Figure 7.** XRD spectra for various samples: clean Al, porous alumina as well as different stage 3 coatings. Undoped sample (6) is presented for comparison.

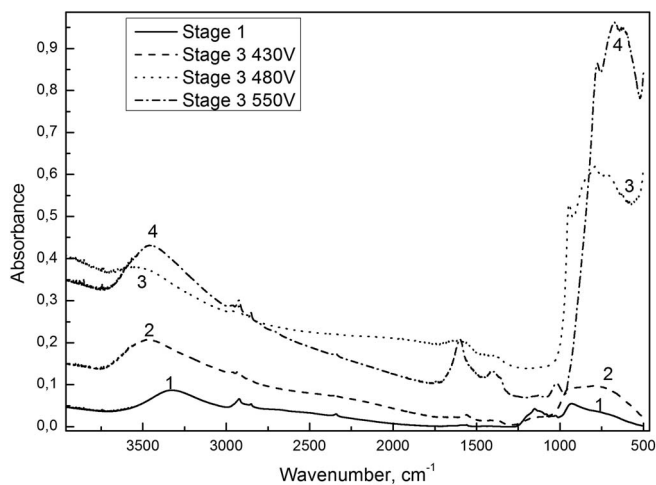


**Figure 8.** FTIR spectra for various PEO samples: 1 – clean porous coating; 2,3 and 4 – Eu filled pores after 430 V, 480 V and 550 V accordingly.

### Conclusions

Europium doped luminescent coatings were produced using PEO process.  $\text{Eu}^{2+}$  ion presence in final coatings was evaluated using various spectral distribution and decay kinetics measurements. Up to 10 times total photoluminescence intensity increase in visible range observed.

During coating deposition process Eu ion recharge from  $\text{Eu}^{3+}$  to  $\text{Eu}^{2+}$  state was observed. This phenomenon might be related to the presence of oxygen vacancies in coatings.

By analyzing coating structure with XRD and FTIR,  $\eta\text{-Al}_2\text{O}_3$  phase was detected. Correlation between  $\eta$ - phase and luminescence properties was established and could be used for phase transition detection.

Overall, authors believe that the presented approach for doping PEO coatings can be applied for many other materials and metals to create coatings with new properties.

### Acknowledgments

Financial support provided by Scientific Research Project for Students and Young Researchers Nr. SJZ2015/21 realized at the Institute of Solid State Physics, University of Latvia is greatly acknowledged.

The authors are grateful to G. Cikvaidze for FTIR measurements, R. Ignatans for measurements and analysis of XRD spectra and ElGoo Tech ltd. for providing various PEO equipment.

### References

1. J. A. Curran and T. W. Clyne, "Thermo-physical properties of plasma electrolytic oxide coatings on aluminum," *Surf. Coatings Technol.*, **199**, 168 (2005).
2. A. L. Yerokhin, V. V. Lyubimov, and R. V. Ashitkov, "Phase formation in ceramic coatings during plasma electrolytic oxidation of aluminum alloys," *Ceram. Int.*, **24**, 1 (1998).

3. U. Malayoglu, K. C. Tekin, U. Malayoglu, and S. Shrestha, "An investigation into the mechanical and tribological properties of plasma electrolytic oxidation and hard-anodized coatings on 6082 aluminum alloy," *Mater. Sci. Eng. A*, **528**, 7451 (2011).
4. A. L. Yerokhin, X. Nie, A. Leyland, A. Matthews, and S. J. Dowey, "Plasma electrolysis for surface engineering," *Surf. Coatings Technol.*, **122**, 73 (1999).
5. K. Du, X. Guo, Q. Guo, Y. Wang, F. Wang, and Y. Tian, "Effect of PEO Coating Microstructure on Corrosion of Al 2024," *J. Electrochem. Soc.*, **159**, C597 (2012).
6. L. Grigorjeva, D. Millers, K. Smits, and A. Zolotarjovs, "Gas sensitive luminescence of ZnO coatings obtained by plasma electrolytic oxidation," *Sensors Actuators A Phys.*, **234**, 290 (2015).
7. L. White, Y. Koo, S. Neralla, J. Sankar, and Y. Yun, "Enhanced mechanical properties and increased corrosion resistance of a biodegradable magnesium alloy by plasma electrolytic oxidation (PEO)," *Mater. Sci. Eng. B*, **208**, 39 (2016).
8. M. Aliofkhaezai and A. S. Rouhaghdam, "Wear and coating removal mechanism of alumina/titania nanocomposite layer fabricated by plasma electrolysis," *Surf. Coatings Technol.*, **205**, S57 (2011).
9. C. Martini, L. Ceschini, F. Tarterini, J. M. Paillard, and J. A. Curran, "PEO layers obtained from mixed aluminate-phosphate baths on Ti-6Al-4V: Dry sliding behaviour and influence of a PTFE topcoat," *Wear*, **269**, 747 (2010).
10. C. S. Dunleavy, J. A. Curran, and T. W. Clyne, "Plasma electrolytic oxidation of aluminum networks to form a metal-cored ceramic composite hybrid material," *Compos. Sci. Technol.*, **71**, 908 (2011).
11. K. Smits, L. Grigorjeva, D. Millers, A. Sarakovskis, A. Opalinska, J. D. Fidelus et al., "Europium doped zirconia luminescence," *Opt. Mater. (Amst.)*, **32**, 827 (2010).
12. E. Elsts, G. Kriekle, U. Rogulis, K. Smits, A. Zolotarjovs, J. Jansons et al., "Rare earth doped glass-ceramics containing NaLaF<sub>4</sub> nanocrystals," *Opt. Mater. (Amst.)*, (2016).
13. I. V. Gasenkova, E. V. Ostapenko, and N. I. Mazurenko, "Optical Properties of Anodic Aluminum Oxide Produced in a Complex Electrolyte," *Journal of Surface Investigation. X-ray, Synchrotron and Neutron Techniques*, **8**, 636 (2014).
14. A. M. Md Jani, D. Losic, and N. H. Voelcker, "Nanoporous anodic aluminum oxide: Advances in surface engineering and emerging applications," *Prog. Mater. Sci.*, **58**, 636 (2013).
15. Z. Zhang, M. Gu, Y. Hu, X. Liu, S. Huang, B. Liu et al., "Template synthesis and luminescence of ordered Lu<sub>3</sub>Al<sub>5</sub>O<sub>12</sub>:Ce<sup>3+</sup> nanowire arrays," *Mater. Lett.*, **166**, 158 (2016).
16. K. Smits, D. Millers, A. Zolotarjovs, R. Drunka, and M. Vanks, "Luminescence of Eu ion in alumina prepared by plasma electrolytic oxidation," *Appl. Surf. Sci.*, **337**, 166 (2015).
17. K. M. Lee, J. O. Jo, E. S. Lee, B. Yoo, and D. H. Shin, "Incorporation of Carbon Nanotubes Into Oxide Layer on 7075 Al Alloy by Plasma Electrolytic Oxidation," *J. Electrochem. Soc.*, **158** C325 (2011).
18. S. Stojadinović, N. Tadić, and R. Vasilčić, "Photoluminescence of Sm<sup>3+</sup> doped ZrO<sub>2</sub> coatings formed by plasma electrolytic oxidation of zirconium," 2016.
19. S. Stojadinović and R. Vasilčić, "Formation and photoluminescence of Eu<sup>3+</sup> doped zirconia coatings formed by plasma electrolytic oxidation," *J. Lumin.*, **176**, 25 (2016).
20. S. Stojadinović, N. Radić, B. Grbić, S. Maletić, P. Stefanov, A. Pačevski et al., "Structural, photoluminescent and photocatalytic properties of TiO<sub>2</sub>:Eu<sup>3+</sup> coatings formed by plasma electrolytic oxidation," *Appl. Surf. Sci.*, **370**, 218 (2016).
21. S. Stojadinović, N. Tadić, and R. Vasilčić, "Photoluminescence of Sm<sup>3+</sup> doped ZrO<sub>2</sub> coatings formed by plasma electrolytic oxidation of zirconium," *Mater. Lett.*, **164**, 329 (2016).
22. Y. Yang, H. Wei, L. Zhang, K. Kisslinger, C. L. Melcher, and Y. Wu, "Blue emission of Eu<sup>2+</sup>-doped translucent alumina," *J. Lumin.*, **168**, 297 (2015).
23. V. Singh, T. K. Gundu Rao, and J.-J. Zhu, "Synthesis, photoluminescence, thermoluminescence and electron spin resonance investigations of CaAl<sub>12</sub>O<sub>19</sub>:Eu phosphor," *J. Lumin.*, **126**, 1 (2007).
24. J. Ueda, T. Shinoda, and S. Tanabe, "Evidence of three different Eu<sup>2+</sup> sites and their luminescence quenching processes in CaAl<sub>2</sub>O<sub>4</sub>:Eu<sup>2+</sup>," *Opt. Mater. (Amst.)*, **41**, 84 (2015).
25. G. Mrówka-Nowotnik, J. Sieniawski, and M. Wierzbńska, "Intermetallic phase particles in 6082 aluminum alloy," *Arch. Mater. Sci. Eng.*, **28**, 69 (2007).
26. S. Gražulis, D. Chateigner, R. T. Downs, A. F. T. Yokochi, M. Quirós, L. Lutterotti et al., "Crystallography Open Database {-} an open-access collection of crystal structures," *J. Appl. Crystallogr.*, **42**, 726 (2009).
27. J. Li, Y. Pan, C. Xiang, Q. Ge, and J. Guo, "Low temperature synthesis of ultrafine ??-Al<sub>2</sub>O<sub>3</sub> powder by a simple aqueous sol-gel process," *Ceram. Int.*, **32**, 587 (2006).